Conductive imprinted polymers for the direct electrochemical detection of β-lactam antibiotics: The case of cefquinome

Giulia Moro[a,b], Fabio Bottari[a], Nick Sleegers[a], Anca Florea[a], Todd Cowen[c], Ligia Maria Moretto[b], Sergey Piletsky[c], Karolien De Wael[a,*]

[a] AXES Research Group, Department of Chemistry, University of Antwerp, Groenenborgerlaan 171, 2020 Antwerp, Belgium
[b] LSE Research Group, Department of Molecular Science and Nanosystems, Università Ca' Foscari, Via Torino 155, 30172, Venice Mestre Italy
[c] University of Leicester, Department of Chemistry, LE1 7RH, UK

ARTICLE INFO

Keywords:
Cefquinome
4-aminobenzoic acid
Molecularly imprinted polymer
Electropolymerization
Biomimetic sensor
Multi-walled carbon nanotubes

ABSTRACT

A biomimetic sensor for cefquinome (CFQ) was designed at multi-walled carbon nanotubes modified graphite screen-printed electrodes (MWCNTs-G-SPEs) as a proof-of-concept for the creation of a sensors array for β-lactam antibiotics detection in milk. The sensitive and selective detection of antibiotic residues in food and environment is a fundamental step in the elaboration of prevention strategies to fight the insurgence of antimicrobial resistance (AMR) as recommended by authorities around the world (EU, WHO, FDA). The detection strategy is based on the characteristic electrochemical fingerprint of the target antibiotic cefquinome. A conductive electropolymerized molecularly imprinted polymer (MIP) coupled with MWCNTs was found to be the optimal electrode modifier, able to provide an increased selectivity and sensitivity for CFQ detection. The design of CFQ-MIP was facilitated by the rational selection of the monomer, 4-aminobenzoic acid (4-ABA). The electropolymerization process of 4-ABA have not been fully elucidated yet; for this reason a thorough study and optimization of electropolymerization conditions was performed to obtain a conductive and stable poly(4-ABA) film. The modified electrodes were characterized by electrochemical impedance spectroscopy (EIS), scanning electron microscopy (SEM) and cyclic voltammetry (CV). CFQ-MIP were synthesized at MWCNT-G-SPEs by electropolymerization in pH ≈ 1 (0.1 M sulphuric acid) with a monomer:template ratio of 5:1. Two different analytical protocols were tested (single and double step detection) to minimize unspecific adsorptions and improve the sensitivity. Under optimal conditions, the lowest CFQ concentration detectable by square wave voltammetry (SWV) at the modified sensor was 50 nM in 0.1 M phosphate buffer pH 2.

1. Introduction

Biomimetic materials, and molecularly imprinted polymers (MIP) in particular, are promising electrode modifiers for the design of electrochemical sensors able to selectively detect numerous food and environmental contaminants [1–3], such as β-lactam antibiotics [4–6]. MIP represent an appealing alternative to bioreceptors (enzymes, antibodies or proteins) thanks to their higher stability, low cost and easy preparation protocol [7]. The synthesis of MIP is characterized by three main steps: (1) the formation of a pre-polymerization complex between the template, i.e. the target molecule, and the functional monomers (*pre-arrangement step*), (2) the (electro) polymerization of the monomer and (3) the subsequent removal of the template (*extraction step*) that leads to the formation of target-specific cavities within the polymeric network. These cavities, complementary in size, shape and chemical functionalities with the template, selectively bind the target molecules, even in presence of structurally related compounds.

In recent years, the use of imprinted polymers for electroanalytical applications gathered considerable attention thanks to the versatility of these electrode modifiers [5,8]: their combination with conductive nanomaterials such as carbon nanotubes, gold nanoparticles or graphene allows to improve greatly the sensitivity [9,10] for electroactive targets as well as non-electroactive ones [11]. The main advantages of imprinted polymers for analytical environmental applications lie in their robustness, the possibility to reduce matrix interferences and the versatility of the possible analytical configurations [12,13]. Moreover, compared to traditional MIP obtained by bulk polymerization, electropolymerized ones do not require an additional immobilization step, a factor that could limit their application in electroanalysis [14–16].

MIP can be directly integrated with the transducer surface by

* Corresponding author.
E-mail address: karolien.dewael@uantwerpen.be (K. De Wael).

https://doi.org/10.1016/j.snb.2019.126786
Received 29 March 2019; Received in revised form 17 June 2019; Accepted 5 July 2019

electropolymerization of the monomer under potentiostatic or potentiodynamic conditions [17]. By varying the electropolymerization working conditions, it is possible to adjust the rate of polymer nucleation and growth, the film thickness and morphology obtaining specific electrochemical properties [18]. The properties of the final polymer mainly depend on the monomer concentration, the electropolymerization technique (potentiostatic or –dynamic) and the electrolyte and solvents used during the polymerization [19,20].

The possibility to obtain an electronically conductive polymer (ECP) is of paramount importance for the detection of electroactive targets because the selectivity provided by the key-and-lock mechanism of the MIP cavities will be coupled with the specific electrochemical signal of the target leading to highly selective biomimetic sensors. The most investigated ECPs are based on pyrrole, 3-aminophenylboronic acid, phenol, thiophenol and aniline [21]. Recently, carboxyl-substituted anilines, known as aminobenzoic acids (ABAs), and in particular 4-ABA, are giving promising results in sensing applications. 4-ABA has been previously employed in chemical sensors [22,23] and biosensor platforms [24–27], electrodeposited anticorrosion coatings [28,29] and as a linkers for polyoxometalates immobilization on glassy carbon electrodes [30]. Despite its numerous applications, the polymerization mechanism of 4-ABA remains unclear [31] and no extensive studies have been dedicated to map the film properties in different electropolymerization conditions. In the present work, the influence of certain electropolymerization parameters such as pH, number of cyclic voltammetry (CV) cycles and monomer concentration was investigated and optimized to obtain a conductive 4-ABA based MIP sensor.

β-lactam residues in milk and other animal tissues are a cause of concern for authorities and consumers: they induce allergic reactions in hypersensitive individuals [32], interfere with the fermentation processes used by dairy industries [33] and contribute to the spreading of antimicrobial resistance [34]. To prevent such consequences, the European Union has established specific threshold values for each drug in food commodities, namely the Maximum Residues Limits (MRLs) [35]. To undertake the monitoring plans prescribed in prevention strategies protocols, it is necessary to design selective, sensitive, portable and cheap analytical tools [36]. In this frame, an array of biomimetic electrochemical sensors represents a promising option between the currently used methods based on chromatographic techniques [37,38] or screening tests [39,40]. To test the feasibility of a biomimetic sensor array based on direct electrochemical detection, cefquinome (CFQ) was chosen as a model target. CFQ is a fourth generation cephalosporin that has a broad-spectrum activity, commercialized for veterinary treatments as Cobactan® and Cephaguard® [41].

To detect nanomolar concentrations and thus reaching MRL levels (MRL_{CFQ} is c.a. 40 nM), biomimetic polymers can be combined with other modifiers such as multi-walled carbon nanotubes (MWCNTs) able to enhance the electron transfer. Other advantages of MWCNTs in electroanalytical applications are related to their high surface area and chemical and physical stability [42]. MWCNTS were successfully applied in other cephalosporins electrochemical sensors, for the determination of cefixime and cefpirome [43,44].

In this work, the electrochemical fingerprint of CFQ was first studied, then the electrochemical properties of 4-ABA polymer were accurately mapped and the MIP synthesis protocol was optimized at MWCNT-G-SPEs. Finally, two different analytical protocols were tested (single and double step detection) and the performances of the final sensor were fully evaluated.

2. Material & methods

2.1. Reagents

Cefquinome sulfate (CFQ) and 4-aminobenzoic acid (4-ABA) were purchased from Sigma-Aldrich Ltd (Belgium); 2-(2-aminothiazole-4-yl)-2-methoxyiminoacetic acid (SC), cefoperazone (CFP), cephalexin (CFX) and ceftiofur (CFU) were obtained from TCI (Europe). Phosphate buffer solutions (PB) 0.1 M were prepared by mixing stock solutions of 0.1 M NaH_2PO_4 and 0.1 M Na_2HPO_4, purchased form Sigma Aldrich, to obtain different pH values and 0.1 M of NaCl was added to obtain the corresponding saline buffer (PBS). To extend the pH range until 3 and 4, suitable amounts of phosphoric acid (H_3PO_4) were added. The PB pH 2 was obtained from phosphoric acid, purchased form Sigma Aldrich. A 0.1 M H_2SO_4 solution was used for the lowest pH value (pH ≈ 1). Stock solutions of 10 mM CFQ in MilliQ water were kept at 4 °C for up to three days. Standard working solutions of CFQ were obtained by dilution of the stock solutions with the suitable buffer. Stock solutions of 10 mM 4-ABA in 0.1 M PBS at pH 7 were prepared every day. All other reagents were of analytical grade and used without further purification. All aqueous solutions were prepared using MilliQ water (R > 18 MΩcm).

2.2. Rational monomer selection

The computational modelling was performed as described by Piletsky et al. [45]. A virtual library of electropolymerizable monomers (≈ 20) was screened using the LEAPFROG™ algorithm (SYBYL® 7.3 software package, Tripos International, USA) to investigate their interaction with the template. Energy minimization was conducted to a minimum of 0.001 kcal mol^{-1} $Å^{-1}$ gradient. The parameters of molecular mechanics were: method Powell, force field Tripos and charges Gasteiger-Huckel. The library of electroactive monomers was ranked depending on the ΔG calculated as the difference between the energy of each ligand-monomer complex and the corresponding energies of the free monomers and the free CFQ. Among the first five monomers which gave the lowest ΔG reported in Table S1, 4-aminobenzoic acid (4-ABA) was selected (ΔG = -104.081 kJ mol^{-1}).

2.3. Electrochemical measurements

CV and SWV were carried out using an Autolab potentiostat/galvanostat (PGSTAT 302 N, ECOCHEMIE, The Netherlands) controlled by NOVA 1.1 software. Graphite screen-printed electrodes, bare (G-SPEs) and modified with multi-walled carbon nanotubes (MWCNT-G-SPEs) were purchased from DropSens (Spain). They are composed of a graphite working electrode (3 mm diameter), a graphite counter electrode and a silver pseudo reference electrode. The following parameters were employed for the electropolymerization of 4-ABA by CV: -0.3 V to +1.2 V potential range, 50 mVs^{-1} scan rate with seven consecutive cycles. CVs used to investigate the CFQ electrochemical fingerprint and its C7 side chain (2-(2-aminothiazole-4-yl)-2-methoxyiminoacetic acid) were performed between 0.0 V and +1.5 V potential range, 50 mVs^{-1} scan rate, 0.1 M PB pH 2. To obtain SWVs of CFQ, the following parameters were used: +0.4 V and +1 V potential range, 5 mV step potential, 25 mV amplitude, 10 Hz frequency. Except where otherwise stated all the potentials are referred to Ag pseudo reference (+200 mV compared to SCE). All electrochemical experiments were performed at room temperature.

2.4. Analytical protocol

For the single step detection (SSD), a drop of 100 µL of PB solution spiked with different CFQ concentrations was left in contact with the electrode for 1 min before running a SWV. For the double step detection (DSD) 50 µL of PB solution spiked with different CFQ concentrations were placed at the modified electrode for various timeframes (1–5 min s) (*step 1*). Afterwards, the drop was removed and the electrode surface was rinsed with 3 mL of MilliQ water and 100 µL of 0.1 M PB pH 2 was placed at the electrode (*step 2*) before running a SWV. All results obtained by SWV are presented after baseline correction using the mathematical algorithm “Moving average” (peak width = 1) contained within NOVA 1.1 software, to improve the visualization and identification of the peaks over the baseline.

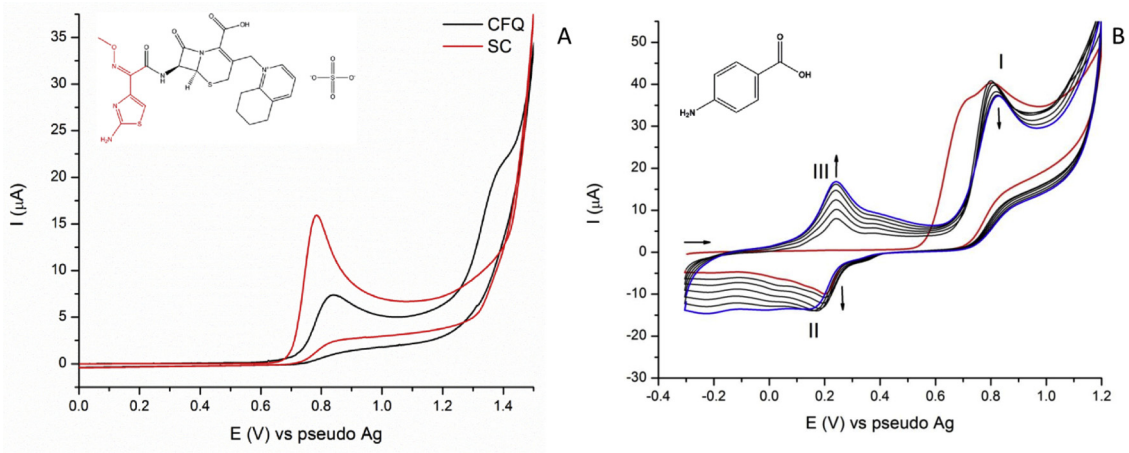

Fig. 1. (A) CVs of individual solutions of 500 μM CFQ and SC in 0.1 M PB pH2 at G-SPEs, 50 mVs^{-1}; inset: CFQ structure with SC in red; (B) CVs obtained for the electropolymerization of 1 mM 4-ABA in 0.1 M H_2SO_4 at MWCNTs-G-SPE, 50 mVs^{-1}. The arrows indicate the direction of the current increase/decrease as a function of the number of CV cycles from the first cycle (red) to the 7th (blue). Inset: 4-aminobenzoic acid structure (For interpretation of the references to colour in this figure legend, the reader is referred to the web version of this article).

2.5. Electrode characterization

The modified electrodes were characterized by SEM and EIS. SEM images were acquired with a Field Emission Gun – Environmental Scanning Electron Microscope equipped with an Energy Dispersive X-Ray detector (FEI Quanta 250, USA). EIS measurements were carried out in 0.1 M PBS pH 7 with 2 mM $[Fe(CN)_6]^{3-/4-}$, in the frequency range between 0.1 MHz and 1 Hz, with 0.01 V amplitude and DC potential determined by Open Circuit Potentials.

3. Results and discussion

3.1. Cefquinome electrochemical behaviour

The electrochemical fingerprint of CFQ at G-SPEs in Fig. 1A was characterized by two irreversible oxidation peaks at +0.7 V and +1.3 V vs pseudo Ag reference electrode. The peak at +1.3 V corresponds to the irreversible oxidation of the cephem nucleus; it is common to all cephalosporins, thus not useful for a selective identification of CFQ [46]. The oxidation peak at +0.7 V (red curve, Fig. 1A) can be ascribed to CFQ C7 side chain (SC) that characterizes only the more recent classes of cephalosporins such as the 3rd and 4th generations. Therefore, it is possible to base CFQ identification directly on the SC signal.

3.2. 4-ABA electropolymerization study

The cyclic voltammograms accounting for the optimized electropolymerization of 4-ABA on MWNTs-G-SPE, in Fig. 1B are characterized by: the monomer region in which 4-ABA is irreversibly oxidized around +0.8 V (I) leading to the formation of radical species (*activated monomers*) and the polymer region between −0.3 V and +0.4 V where the redox peaks (II and III) allow to follow the polymer growth [24].

In the first cycle (red line, Fig. 1B), the monomer peak was preceded by a shoulder at +0.7 V that could be ascribed to the adsorption of the neutral monomer at the electrode surface before its oxidation [47] or to the formation of different highly-reactive radicals [24]. Increasing the number of cycles, the anodic peak current of the monomer (I) decreases, showing the progressive oxidation of the monomer at the electrode surface. The main polymer redox peaks showed an E_{pc} of +0.17 V (II) and an E_{pa} of +0.23 V (III) in the last voltammogram (blue line, Fig. 1B); both peaks showed increasing currents (II and III) upon increasing number of CV cycles. The constant increase of the polymer peak currents together with the decrease in the monomer peak current testifies the constant and surface controlled nature of the modification, while maintaining the electrode surface conductivity.

A thorough study of the 4-ABA electropolymerization was then performed on bare G-SPEs before reaching the optimal conditions (see Fig. 1B) aiming to map the polymer properties and to optimize the main parameters involved, namely the pH, the scan rate, the monomer concentration and the number of CV cycles.

3.2.1. Optimization of the pH

A pH study from 1 to 7 was performed to map the pH dependent behaviour of 4-ABA and to choose the optimal value to obtain a conductive and stable modification (Fig. S.1A–G). Comparing the peak currents of the polymer, it was observed that for pH 2 to 6 the polymer growth seems faster than at pH 1 and 7. At pH 2, 3 and 6 the polymer peaks (II and III in Fig. 1B) remained constant after five CV cycles. At pH 4 and 5 both peaks II and III started decreasing after three cycles with a clear overlap in both oxidation and reduction peaks. The pH influence was evident also considering the peak potential shifts: the polymer E_{pc} was +0.17 V at pH 7 and +0.55 V at pH 1 (see Fig. S.1.G and A). These observations were justified considering the amphiprotic nature of 4-ABA whose functional groups can be protonated or deprotonated depending on the pH of the electrolyte (pK_{a1} = 2.38, pK_{a2} = 4.85 at 25 °C [48,49]). In the pH range 2 to 6, the heterogeneous forms of the functional groups could enhance the polymerization rate, while at pH 1 and 7 the monomers are completely protonated or deprotonated resulting in a slower, but monotonic polymer growth.

Aiming to perform surface controlled polymerization, the relationship between the peak current and the number of cycles was accurately evaluated (see Fig. 2). Only at pH 1 and pH 7 the polymer showed a gradual growth resulting in an increased oxidation and reduction currents (peaks II and III in Fig. 1B) while in 2–6 pH range (with pH 5 shown in Fig. 2) a decrease in the same currents after the first few CV cycles suggests the formation of a thicker and less conductive layer. This behaviour is in agreement with many electropolymerization mechanisms reported for other electroactive monomers [50–52].

Despite the fast growth observed using pH from 2 to 6, these pH values were discarded because of the difficulty in controlling the film electrochemical properties. The passivating effect, evident from the decrease of the current of the polymer peaks, was deemed not suitable to monitor the effect of other parameters (e.g. monomer: template ratio) on the conductivity of the obtained film. Differences in the peak current and potential of the polymers peaks can thus be used as an indication of the effect of the MIP protocol optimization on the

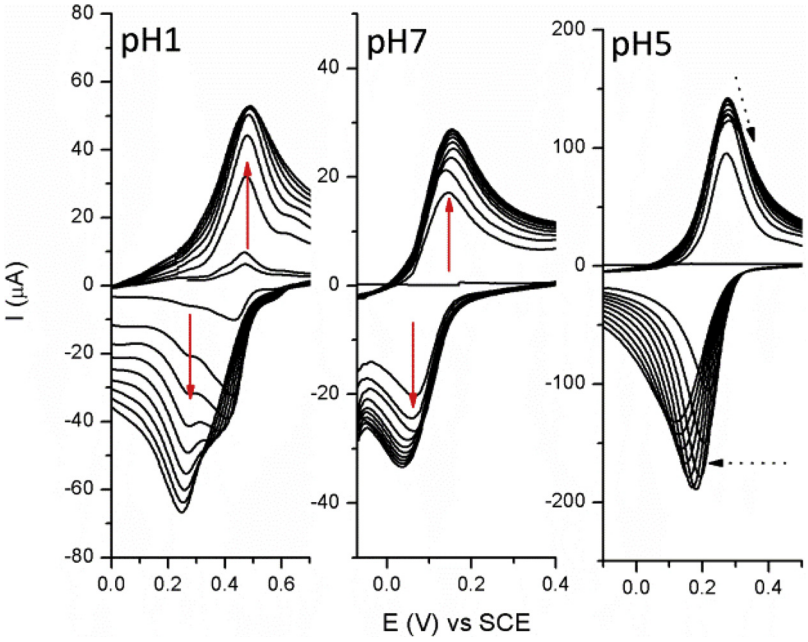

Fig. 2. Focus on polymers I_{pa} and I_{pc} for the electropolymerization of 4-ABA (from left to right) at pH 1, 7, 5; 10 consecutive cycles of CV at 50 mVs^{-1} for 1 mM 4-ABA at G-SPE.

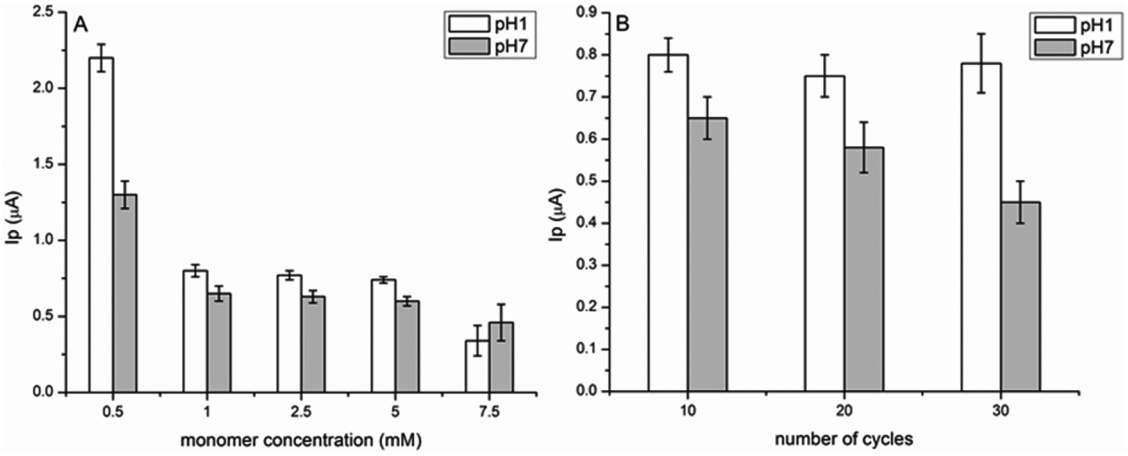

Fig. 3. Comparison of peak currents of CFQ (50 μM) at G-SPEs modified with 4-ABA using: (A) different monomer concentrations or (B) different numbers of CV cycles during the electropolymerization.

obtained polymer (see Section 3.2.2). For the same reasons, both pH 1 and pH 7 were considered suitable for the present application and further tested in the following optimization study, expecting different responses because of the different ionic species involved during electropolymerization.

3.2.2. Optimization of scan rate, monomer concentration and number of CV cycles

A literature survey allowed to identify the most commonly used parameters for scan rates, monomer concentrations and number of CV cycles [23,24]. These parameters were tested following a one-variable-at-a-time approach (OVAT), keeping constant the other two. The first criterion considered in the selection of the optimal value of a parameter was the consistency of the electropolymerization voltammograms with the standard presented in Fig. 1B, upon changing the investigated parameter. If no discernible differences in the voltammograms pattern were identified, the selected subset of parameters was further compared using the oxidation signal of 50 μM CFQ to select the best value for each parameter.

The second selection criterion was based on the expected CFQ response (oxidation peak at +0.7 V vs pseudo Ag) and a sensible difference in its intensity (Ip) between the bare and the 4-ABA modified electrode. Indeed, CFQ oxidation should be detectable in the presence of a stable conductive modification giving a less intense signal if compared to bare electrodes. The decrease in signal can be used as an indication that the film formed on the surface is thick enough to host imprinted cavities while still maintaining good conductivity and allowing the ET with the antibiotic.

The first parameter studied was the scan rate: literature [7,8] gives values of 50 or 100 mVs^{-1} for electropolymerization, thus these two values were tested at both pH (1 and 7). Scan rate of 50 mVs^{-1} showed a evident difference between the bare and the modified electrode signal (Ip = 1.4 μA at G-SPE and an Ip = 0.8 μA at 4-ABA modified G-SPE, for 50 μM CFQ) with a smaller STD. At 100 mVs^{-1}, the peaks of the polymer in the electropolymerization CVs showed a behaviour similar to the one of intermediate pH values (see Section 3.2.1) with overlaps after a few cycles of electropolymerization. Thus, 50 mVs^{-1} was chosen as the optimal scan rate value; indeed increasing the scan rate of the

electropolymerization CVs has been proven to result in an increase in ΔEp of the polymer peak indicating a less reversible system [53].

Considering the monomer concentration, the tested values were: 0.5, 1, 2.5, 5 and 7.5 mM (see Fig. 3A). The performances of intermediate concentrations (1, 2.5, 5 mM) were found to be comparable with an associated error of 4% at pH 1 and 6% at pH 7 on average, while the lowest and highest monomer concentrations gave sensibly different responses. The films with 7.5 mM of 4-ABA provided signals with an intensity three times lower in comparison to intermediate monomer concentrations in acid conditions while at pH 7 a smaller difference was recorded (≈ 0.1 μA). The results obtained for 0.5 mM were very similar to the ones recorded at bare electrodes suggesting that the films were probably too thin and inhomogeneous to form stable target-specific cavities. Thus, the 7.5 mM and the 0.5 mM were discarded and only the intermediate monomer concentrations were found to be suitable for these kind of modifications. Considering the two pHs, in all cases, pH 1 gave better results in terms of CFQ signal intensity and reproducibility. From the present study, the electropolymerization of 1 mM 4-ABA solution at pH 1 appeared to be the optimal combination to obtain a conductive film with a good balance between reproducibility and CFQ signal intensity.

Keeping 4-ABA concentration fixed at 1 mM, the electropolymerization was performed at 10, 20 and 30 consecutive CV cycles. For all the three values, a good agreement with the standard electropolymerization pattern in Fig. 1B and no significant differences in the SSD results (Fig. 3B) were found. Thus, the lower value, 10 cycles, was chosen to reduce the total protocol time.

The final optimal conditions for 4-ABA electropolymerization at G-SPEs were: 50 mVs^{-1} scan rate, 1 mM monomer concentration and 10 CV cycles.

3.3. MWCNTs

After having optimized the main electropolymerization conditions and before the CFQ-MIP synthesis design, the possibility to integrate MWCNTs was evaluated. The voltammetric response of CFQ solutions at different concentrations was recorded at MWCNTs-G-SPEs. An increase in the faradic peak currents of 40% compared to the bare G-SPE was observed (see Fig. S.2A). The lowest detectable concentration decreased from 0.5 to 0.1 μM in 0.1 M PB pH 2. Aiming to monitor nanomolar CFQ concentrations the improvement of the signal provided by these modifiers was considered fundamental.

Switching from G-SPEs to the MWCNTs-G-SPEs, further tests of the electropolymerization conditions were needed. The number of CV cycles was reduced from 10 to 7. Indeed, after 7 CV cycles on MWCNTs-G-SPEs the redox peaks of the polymer showed an overlapped pattern similar to the result reported for intermediate pH value (2–6) for the study of 4-ABA electropolymerization (see Section 3.2.1). As already concluded, this overlap is indicative of a less conductive modification [51,52]. This behaviour could be ascribed to the improved conductivity and active area provided by the MWCNTs which promoted the growth of the polymer on the electrode.

The MWCNTs-G-SPEs modified with poly(4-ABA) were characterized by SEM analysis, CV and EIS. From the SEM image in Fig. 4B, it is possible to observe that the MWCNTs are partially wrapped by a smooth polymer layer (see Fig. 4A). CVs in presence of 2 mM $[Fe(CN_6)]^{3-/4-}$ confirmed that the deposition was successful and that the electrode surface is still conductive. Looking at the CV (full line in Fig. 4C) it is possible to see that, after the electropolymerization, the ΔEp increases (˜220 mV) and the peaks are broader compared to the bare electrode (dashed line in Fig. 4C). In addition, the Nyquist plot in Fig. 4D indicates that the deposition was successful, registering an increase in the semi-circular area of the spectrum at higher frequencies, related to the charge transfer resistance on the electrode surface.

3.4. CFQ-MIP synthesis protocol on MWCNTs-SPE

To finalize the design of CFQ-MIP, two other important set of parameters were taken into account: the monomer:template ratio and the parameters for the extraction procedure, both in terms of solvent and extraction time. The optimal value for each parameter was selected comparing the performances of the film after the CFQ rebinding in term of oxidation signal intensity and reproducibility. The rebinding of the target was performed by allowing a drop of the target solution in PB (50 μM) in contact with the modified electrode for 2 min, before rinsing with MilliQ water to remove unspecific adsorbed species and finally running a SWV in a fresh microvolume of 0.1 M PB pH 2 to detect the oxidation signal of CFQ. As a comparison, non-imprinted polymers (NIP) were also synthesized using the same protocol without the addition of the target template and used as a control to verify the success of the imprinting approach. Concerning the monomer:template ratio, two values, 5:1 and 3:1, were studied. Preliminary tests suggested that with higher ratios (10:1) a lower number of cavities were created, while with lower ratios (1:1, 2:1) unstable modifications were obtained. Instead, both 5:1 and 3:1 ratios gave stable modifications with a significant difference in MIP and NIP responses in terms of signal reproducibility. The results showed that the 3:1 ratio gave an average current intensity higher than the 5:1, but it was less reproducible with an error of 12% against the 6% of the 5:1 (see Fig. S3). Reproducibility being a fundamental issue for the proposed modification, the monomer:template ratio 5:1 was chosen as the best alternative. The effect of the template in polymerization solution was also ascertained looking at the electropolymerization CVs for both MIP and NIP (electropolymerization patterns reported in Fig. S4). The voltammetric pattern is the same for both modified sensors: the only difference is the absence of the shoulder at + 0.7 V (see also Fig. 1B) in the first cycle for the MIP. Thus we may conclude that the presence of the template does not hinder the formation of the 4-ABA film on the electrode surface. The extraction step aims to remove the template without interfering with the architecture of the polymeric network and to allow the rebinding of the target. To design this step, warm (˜60 °C) and RT MilliQ water, water:acetonitrile (4:1) and 0.1 M PB pH 12 were tested as extraction solvents with a fixed extraction time of 5 min. As underlined in Fig. 5A, only the extraction in 0.1 M PB pH 12 assured a complete removal of the template. Using the other extraction solutions, CFQ remained partially entrapped as can be seen by the presence of its electrochemical signal after the extraction. Moreover, the 0.1 M PB pH 12 did not hamper the detection of the CFQ after the rebinding. The corresponding signal (0.84 μA) was higher than the one obtained with RT (0.68 μA) and warm MilliQ water (0.76 μA). In presence of water:acetonitrile (4:1), the increased signal observed was ascribed to the presence of template residues interacting with the solvent.

Different extraction times (t_{ex} = 2, 5, 10, 15 min) were tested using 0.1 M PB pH 12 as extraction solution and the results were compared with the ones obtained on the corresponding NIP (see Fig. 5B) for the rebinding of 50 μM of CFQ. At t_{ex} lower than 10 min, the CFQ signal was lower than expected because of an incomplete removal of the template. At t_{ex} higher than 10 min no difference was observable and the CFQ signal remained stable for longer extraction times. Thus, an extraction step of 10 min in 0.1 M PB pH 12 was chosen. Also the difference between MIP and NIP responses was evident for t_{ex} equal or higher than 10 min. This behaviour can be explained by the presence of the target-mimetic cavities on the MIP which are free to rebind the target, while for the NIP the signal is only due to non-specific adsorption on the polymeric network which is not influenced by the extraction step.

To avoid shifts in the CFQ peak potential and poorly reproducible results (due to the presence of an unchecked pH in the MIP polymeric network), an additional conditioning step was performed after the extraction, consisting in the incubation of a 100 μL drop of 0.1 M PB pH 2 at the modified electrode for 1 min.

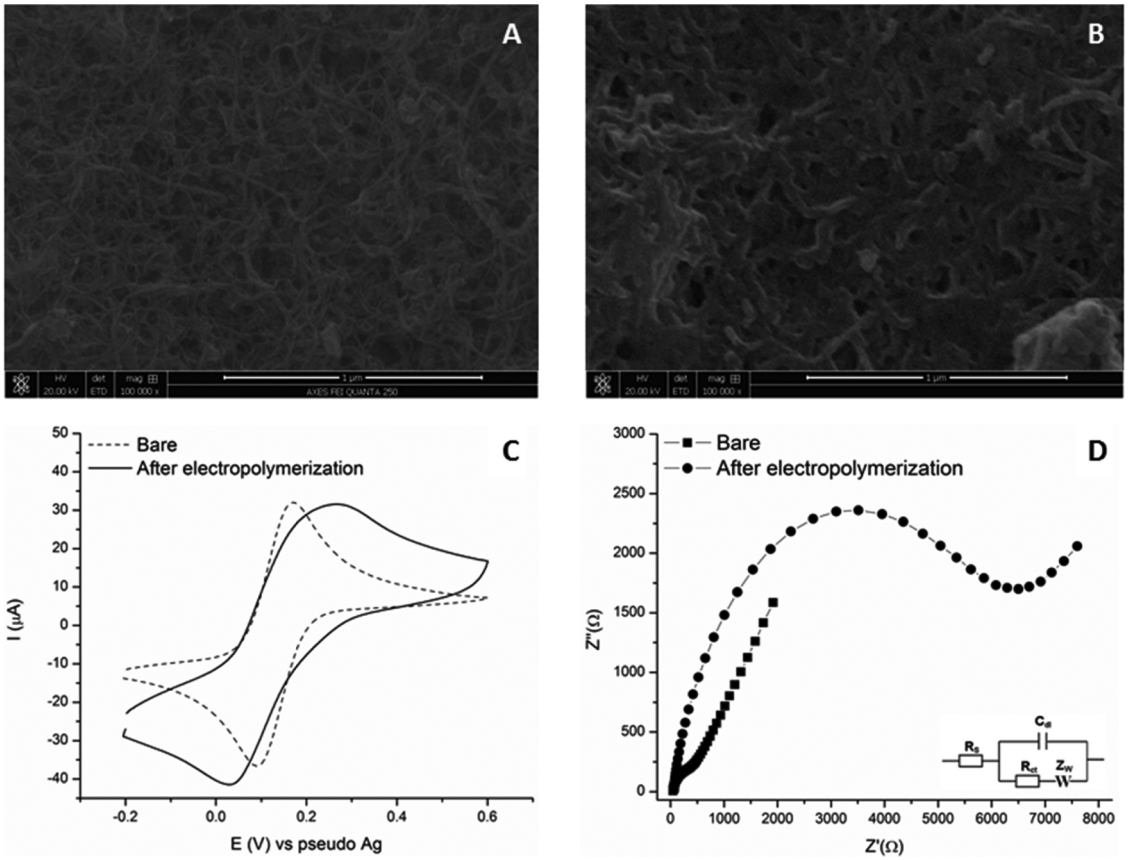

Fig. 4. (A) SEM images of bare MWCNTs-G-SPEs and (B) 4-ABA- MWCNTs-G-SPEs; (C) CV of 2 mM $[Fe(CN)_6]^{3-/4-}$ in 0.1 PBS pH 7 for bare MWCNTs-SPE, 50 mVs^{-1} (dashed line) and 4-ABA-MWCNTs-SPE (full line); (D) Nyquist plot for 2 mM $[Fe(CN)_6]^{3-/4-}$ in 0.1 PBS pH 7 at bare MWCNTs-G-SPEs (square) and 4-ABA-MWCNTs-SPE (dots), inset: Randles equivalent circuit used to fit the data.

The final CFQ-MIP synthesis protocol involved the following steps:

1 Pre-incubation of the electropolymerization solution of 1 mM 4-ABA and 0.2 mM CFQ in 0.1 M H_2SO_4 pH 1 for 10 min.
2 Electropolymerization at the MWCNT-G-SPEs for 7 CV cycles, from -0.3 V to $+1.2$ V at 50 mVs^{-1}.
3 Rinse with 3 mL of MilliQ water and perform a 10 min template extraction with 100 μL of 0.1 M PB pH 12.
4 The modified electrode was rinsed and incubated for 1 min with 100 μL of 0.1 M PB pH 2 before the rebinding.

The modified electrodes were thus ready for the rebinding step.

3.5. Analytical protocol and calibration plot

The performances of two different detection strategies, the SSD and the DSD described in part. 2.4, were compared to find the most suitable analytical protocol. The two protocols were compared considering the

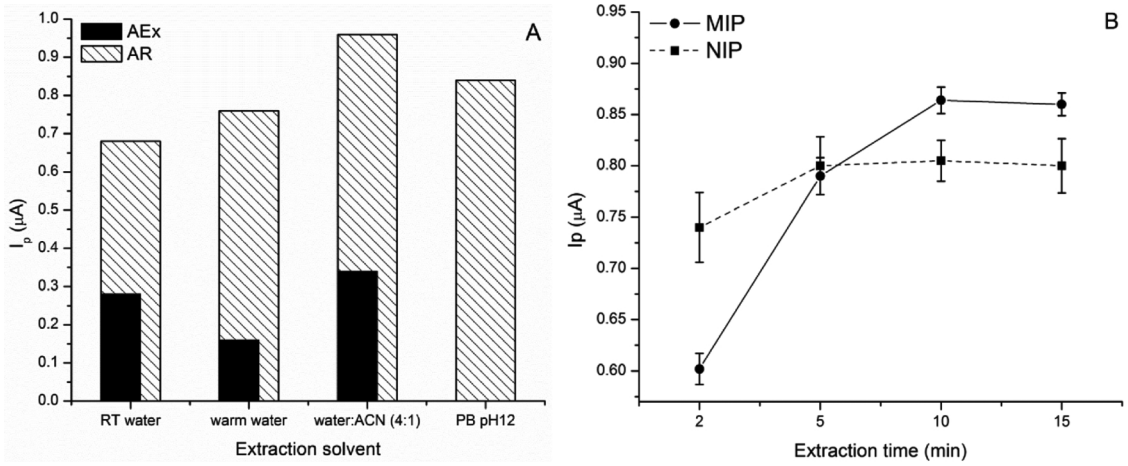

Fig. 5. (A) Comparison of performances after rebinding of 50 μM CFQ in 0.1 M PB pH 2 using different extraction solvents for MIP AEx: after extraction, AR: after rebinding, extraction time 5 min; (B) Signal intensity of 50 μM of CFQ after rebinding with different incubation times for the extraction step with 0.1 M PB pH 12 for MIP and NIP. Error bars calculated on triplicates.

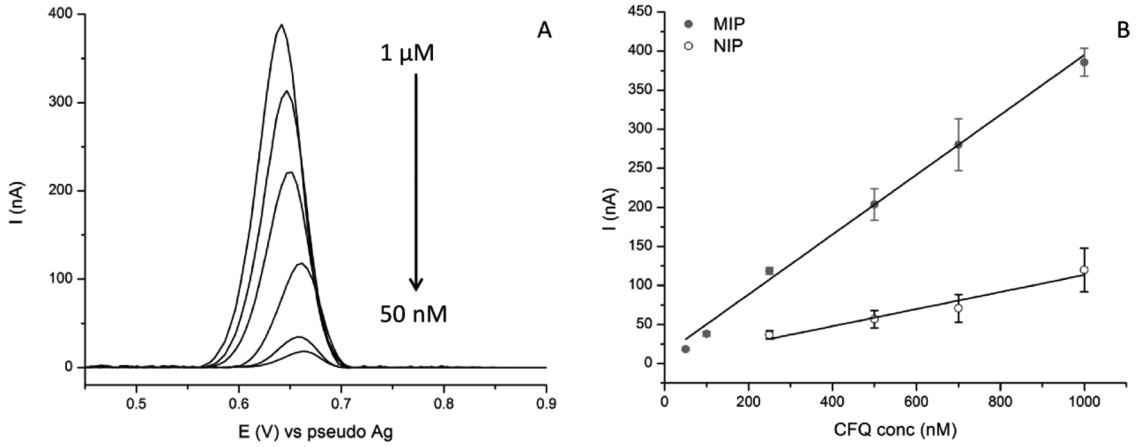

Fig. 6. (A) SWVs of different concentrations (50, 100, 250, 500, 700 and 1000 nM) of CFQ on MIP-MWCNT-G-SPEs and (B) calibration plots obtained with DSD for MIP (grey full dots) and NIP (empty white dots).

differences between the MIP and the NIP responses. By applying SSD, this difference appears to be negligible for all tested concentrations and CFQ concentrations lower than 10 µM were not detectable. On the contrary, using the DSD the signal intensity results were higher for MIP than NIP modified sensors. This difference became relevant when nanomolar concentrations were considered, i.e. at 0.1 µM the CFQ signal was only visible when using the MIP modified electrodes. Thus, nanomolar CFQ concentrations ($\leq$100 nM) were detectable only using the MIP-MWCNT-G-SPEs coupled with a DSD, while the NIP was not able to detect such low concentrations of CFQ. Moreover, this approach proved to be more reliable, reducing the non-specific absorption on the polymer network and increasing the response of the MIP for concentration in the nanomolar range.

With the DSD approach it was possible to obtain a calibration plot for CFQ between 50 nM and 1 u M (see Fig. 6) in 0.1 M PB pH 2 and also the sensor's reproducibility was satisfying (STD < 5% at 4 different electrodes). The corresponding calibration plot at the NIP modified electrode shows first of all that the imprinted sensor is capable of reaching lower concentrations while the NIP is not capable of detecting concentrations lower than 250 nM. The imprinting factor (IF), calculated dividing the slope of the linear fit of the MIP with the one of the NIP, is 3.5.

3.6. Interference study

To test the selectivity of the proposed sensor towards CFQ, three other electroactive cephalosporins [46] used in cattle treatment (namely CFU, CFX and CFP) were analysed at MIP and NIP sensors using the DSD protocol and 1 µM spiked solutions. Especially the response of CFU, a third generation cephalosporin that differs from CFQ only in the C3 side chain (Fig. S5), was assessed on both MIP and NIP modified electrodes. It is worth reminding that CFU is the only other cephalosporin licensed for cattle treatment that has the same active side chain as CFQ. As can be seen from Fig. 7, CFX and CFP gave no signal on both the MIP and the NIP at the oxidation potential of CFQ (+0.7 V vs pseudo Ag). For CFU the response is the same for MIP and NIP (220 nA); this can be explained by the non-specific interaction of the antibiotics with the sensor. This is a first hint of the specificity of the MIP cavities. For CFQ instead the signal for 1 µM is higher on the MIP (380 nA) than the NIP (250 nA) with a lower associated error. The very high standard deviation on the NIP is due to the employed detection strategy, the DSD described in part. 2.4: the rebinding step, performed removing the spiked solution from the electrode and placing a fresh drop of buffer, make the subsequent detection on non-imprinted electrodes less reproducible. The cavities of the MIP selectively capture the antibiotics on the electrode surface, while the NIP signal is only due to non-specific interaction between the bulk polymer and the targets, which can vary sensibly between different analysis.

The proposed modification is also capable of distinguishing between the native and degraded form of CFQ. The signal for 1 µM of CFQ after 24 h of basic degradation at pH 12 on MIP and NIP is almost the same (~ 50 nA). It is worth reminding that the MRLs value are referred to pharmacologically active form of the antibiotics, so the proposed modified sensor shown better selectivity toward the native form of the antibiotic.

4. Conclusions

The proposed MIP for CFQ has shown, first of all, the potentialities of the chosen research methodology regarding the MIP protocol optimization and on the other hand the synergistic effect between nanomaterials and direct electrochemical detection of contaminants. It was indeed possible to obtain an electronically conductive MIP using 4-ABA as functional monomer, elucidating its electrochemical behaviour in a wide range of pHs. The findings about the effects of the pH on the conductivity and the film performances of poly(4-ABA) can be easily exploited also in other applications such as coatings for microchips or batteries. The electopolymerization at pH 1 was proven to be the best choice to obtain conductive polymers and stable molecularly imprinted cavities. Moreover, CFQ identification can be based on the signal of its C7 side chain; the specificity of the electrochemical signal combined with the selectivity of the MIP permitted to distinguish between closely related compounds and more important between intact and degraded from of the antibiotic. A further improvement in the electrode surface modifiers, such as the integration of additional nanomaterials, would allow to reach CFQ concentrations even lower than the MRL value and focus on real sample analysis. Nevertheless, the modified electrode already possess the qualities required for a successful technological transfer and for on-site applications.

Authors contribution

Giulia Moro: Conceptualization, Methodology, Investigation, Validation, Writing – Original Draft, Visualization.

Fabio Bottari: Conceptualization, Methodology, Investigation, Validation, Writing – Review & Editing, Visualization.

Nick Sleegers: Validation, Investigation, Writing – Review & Editing

Anca Florea: Conceptualization, Methodology, Writing – Review & Editing

Todd Cowen: Formal Analysis

Ligia Maria Moretto: Writing – Review & Editing, Supervision

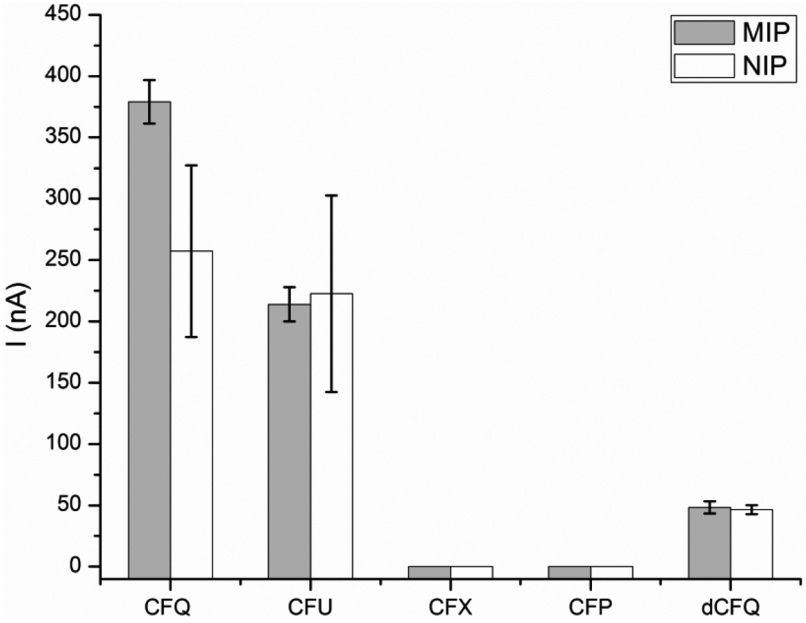

Fig. 7. Interference study: response of 1 μM of cefquinome (CFQ), ceftiofur (CFU), cephalexin (CFX), cefoperazone (CFP) and degraded CFQ (dCFQ) for MIP-MWCNTs-SPE and NIP-MWCNTs-SPE in 0.1 M PB pH2.

Sergey Piletsky: Formal Analysis
Karolien De Wael: Writing – Review & Editing, Supervision

Acknowledgements

This project has received funding from the European Union's Horizon 2020 research and innovation programme under the Marie Skłodowska-Curie Grant Agreement No. 753223. This work was also supported by FWO.

Appendix A. Supplementary data

Supplementary material related to this article can be found, in the online version, at doi:https://doi.org/10.1016/j.snb.2019.126786.

References

[1] S. Ansari, Application of magnetic molecularly imprinted polymer as a versatile and highly selective tool in food and environmental analysis: recent developments and trends, TrAC - Trends Anal. Chem. 90 (2017) 89–106, https://doi.org/10.1016/j.trac.2017.03.001.
[2] S. Boulanouar, S. Mezzache, A. Combès, V. Pichon, Molecularly imprinted polymers for the determination of organophosphorus pesticides in complex samples, Talanta. 176 (2018) 465–478, https://doi.org/10.1016/j.talanta.2017.08.067.
[3] N. Karimian, A.M. Stortini, L.M. Moretto, C. Costantino, S. Bogialli, P. Ugo, Electrochemosensor for trace analysis of perfluorooctanesulfonate in water based on a molecularly imprinted poly(o-phenylenediamine) polymer, ACS Sens. 3 (2018) 1291–1298, https://doi.org/10.1021/acssensors.8b00154.
[4] J.O. Mahony, K. Nolan, M.R. Smyth, B. Mizaikoff, Molecularly imprinted polymers—potential and challenges in analytical chemistry, Anal. Chim. Acta 534 (2005) 31–39, https://doi.org/10.1016/j.aca.2004.07.043.
[5] O.S. Ahmad, T.S. Bedwell, C. Esen, A. Garcia-Cruz, S.A. Piletsky, Molecularly imprinted polymers in electrochemical and optical sensors, Trends Biotechnol. 37 (2019) 294–309, https://doi.org/10.1016/j.tibtech.2018.08.009.
[6] C. Chen, J. Luo, C. Li, M. Ma, W. Yu, J. Shen, Z. Wang, Molecularly imprinted polymer as an antibody substitution in pseudo-immunoassays for chemical contaminants in food and environmental samples, J. Agric. Food Chem. 66 (2018) 2561–2571, https://doi.org/10.1021/acs.jafc.7b05577.
[7] G. Yang, F. Zhao, Molecularly imprinted polymer grown on multiwalled carbon nanotube surface for the sensitive electrochemical determination of amoxicillin, Electrochim. Acta 174 (2015) 33–40, https://doi.org/10.1016/j.electacta.2015.05.156.
[8] F.W. Scheller, X. Zhang, A. Yarman, U. Wollenberger, R.E. Gyurcsányi, Molecularly imprinted polymer-based electrochemical sensors for biopolymers, Curr. Opin. Electrochem. 14 (2019) 53–59, https://doi.org/10.1016/j.coelec.2018.12.005.
[9] A.A. Lahcen, A. Amine, Recent advances in electrochemical sensors based on molecularly imprinted polymers and nanomaterials, Electroanalysis 31 (2019) 188–201, https://doi.org/10.1002/elan.201800623.
[10] B. Yang, C. Fu, J. Li, G. Xu, Frontiers in highly sensitive molecularly imprinted electrochemical sensors: challenges and strategies, TrAC - Trends Anal. Chem. 105 (2018) 52–67, https://doi.org/10.1016/j.trac.2018.04.011.
[11] G. Moro, K. De Wael, L.M. Moretto, Challenges in the electrochemical (bio)sensing of non-electroactive food and environmental contaminants, Curr. Opin. Electrochem. 16 (2019) 57–65, https://doi.org/10.1016/j.coelec.2019.04.019.
[12] A. Martín-Esteban, Recent molecularly imprinted polymer-based sample preparation techniques in environmental analysis, Trends Environ. Anal. Chem. 9 (2016) 8–14, https://doi.org/10.1016/j.teac.2016.01.001.
[13] A. Speltini, A. Scalabrini, F. Maraschi, M. Sturini, A. Profumo, Newest applications of molecularly imprinted polymers for extraction of contaminants from environmental and food matrices: a review, Anal. Chim. Acta 974 (2017) 1–26, https://doi.org/10.1016/j.aca.2017.04.042.
[14] R. Gui, H. Jin, H. Guo, Z. Wang, Recent advances and future prospects in molecularly imprinted polymers-based electrochemical biosensors, Biosens. Bioelectron. 100 (2018) 56–70, https://doi.org/10.1016/j.bios.2017.08.058.
[15] N. Alizadeh, A. Salimi, Ultrasensitive bioaffinity electrochemical sensors: advances and new perspectives, Electroanalysis. 30 (2018) 2803–2840, https://doi.org/10.1002/elan.201800598.
[16] P. Yáñez-Sedeño, S. Campuzano, J.M. Pingarrón, Electrochemical sensors based on magnetic molecularly imprinted polymers: a review, Anal. Chim. Acta 960 (2017) 1–17, https://doi.org/10.1016/j.aca.2017.01.003.
[17] C. Malitesta, E. Mazzotta, R.A. Picca, A. Poma, I. Chianella, S.A. Piletsky, MIP sensors - the electrochemical approach, Anal. Bioanal. Chem. 402 (2012) 1827–1846, https://doi.org/10.1007/s00216-011-5405-5.
[18] E.V. Piletska, A.R. Guerreiro, M.J. Whitcombe, S.A. Piletsky, Influence of the polymerization conditions on the performance of molecularly imprinted polymers, Macromolecules. 42 (2009), https://doi.org/10.1021/ma900432z.
[19] J. Heinze, Electronically conducting polymers, Top. Curr. Chem. 152 (1990) 1–47, https://doi.org/10.1007/BFb0034363.
[20] M.H. Naveen, N.G. Gurudatt, Y.B. Shim, Applications of conducting polymer composites to electrochemical sensors: a review, Appl. Mater. Today. 9 (2017) 419–433, https://doi.org/10.1016/j.apmt.2017.09.001.
[21] X.G. Li, M.R. Huang, W. Duan, Y.L. Yang, Novel multifunctional polymers from aromatic diamines by oxidative polymerizations, Chem. Rev. 102 (2002) 2925–3030, https://doi.org/10.1021/cr010423z.
[22] J.G. Pacheco, P. Rebelo, F. Cagide, L.M. Gonçalves, F. Borges, J.A. Rodrigues, C. Delerue-Matos, Electrochemical sensing of the thyroid hormone thyronamine (T0AM) via molecular imprinted polymers (MIPs), Talanta. 194 (2019) 689–696, https://doi.org/10.1016/j.talanta.2018.10.090.
[23] F. Lopes, J.G. Pacheco, P. Rebelo, C. Delerue-Matos, Molecularly imprinted electrochemical sensor prepared on a screen printed carbon electrode for naloxone detection, Sensors Actuators, B Chem. 243 (2017) 745–752, https://doi.org/10.1016/j.snb.2016.12.031.
[24] L.F. Ferreira, C.C. Santos, F.S. da Cruz, R.A.M.S. Correa, R.M. Verly, L.M. Da Silva, Preparation, characterization, and application in biosensors of functionalized platforms with poly(4-aminobenzoic acid), J. Mater. Sci. 50 (2015) 1103–1116, https://doi.org/10.1007/s10853-014-8667-4.
[25] F. Ma, Y. Chen, Y. Zhu, J. Liu, Electrogenerated chemiluminescence biosensor for detection of mercury (II) ion via target-triggered manipulation of DNA three-way junctions, Talanta. 194 (2019) 114–118, https://doi.org/10.1016/j.talanta.2018.

10.004.
[26] M. Shamsipur, L. Samandari, A. Taherpour, A. Pashabadi, Sub-femtomolar detection of HIV-1 gene using DNA immobilized on composite platform reinforced by a conductive polymer sandwiched between two nanostructured layers: a solid signal-amplification strategy, Anal. Chim. Acta 1055 (2019) 7–16, https://doi.org/10.1016/j.aca.2018.12.013.
[27] S. Guerrero, L. Agüí, P. Yáñez-Sedeño, J.M. Pingarrón, Oxidative grafting vs. Monolayers self-assembling on gold surface for the preparation of electrochemical immunosensors. Application to the determination of peptide YY, Talanta 193 (2019) 139–145, https://doi.org/10.1016/j.talanta.2018.09.089.
[28] L. Adamczyk, A. Pietrusiak, H. Bala, Corrosion resistance of stainless steel covered by 4-aminobenzoic acid films, Cent. Eur. J. Chem. 10 (2012) 1657–1668, https://doi.org/10.2478/s11532-012-0082-6.
[29] A. Yadav, R. Kumar, H.K. Choudhary, B. Sahoo, Graphene-oxide coating for corrosion protection of iron particles in saline water, Carbon 140 (2018) 477–487, https://doi.org/10.1016/j.carbon.2018.08.062.
[30] J. Liu, L. Cheng, B. Liu, S. Dong, Covalent modification of a glassy carbon surface by 4-aminobenzoic acid and its application in fabrication of a polyoxometalates-consisting monolayer and multilayer films, Langmuir. 16 (2000) 7471–7476, https://doi.org/10.1021/la9913506.
[31] C. Thiemann, C.M.A. Brett, Electrosynthesis and properties of conducting polymers derived from aminobenzoic acids and from aminobenzoic acids and aniline, Synth. Met. 123 (2001) 1–9, https://doi.org/10.1016/S0379-6779(00)00364-7.
[32] FAO, Milk and Dairy Products in Human Nutrition, (2013), https://doi.org/10.1186/1471-2458-11-95.
[33] B. Novés, C. Librán, C.C. Licón, M.P. Molina, A. Molina, M.I. Berruga, Technological failures caused by cephalexin in set-type sheeps milk yogurt, CYTA - J. Food. 13 (2015) 408–414, https://doi.org/10.1080/19476337.2014.990519.
[34] WHO (World Health Organization), Global Action Plan on Antimicrobial Resistance, WHO Libr. Cat. Data Glob., 2015.
[35] Commission regulation (EU) No 37/2010, n.d.
[36] F. Bottari, R. Blust, K. De Wael, Bio(inspired) strategies for the electro-sensing of β-lactam antibiotics, Curr. Opin. Electrochem. 10 (2018) 136–142, https://doi.org/10.1016/j.coelec.2018.05.015.
[37] F.J. Lara, M. del Olmo-Iruela, C. Cruces-Blanco, C. Quesada-Molina, A.M. García-Campaña, Advances in the determination of β-lactam antibiotics by liquid chromatography, TrAC Trends Anal. Chem. 38 (2012) 52–66, https://doi.org/10.1016/J.TRAC.2012.03.020.
[38] D. Barcelo, M. Farré, Analytical methodologies for the detection of β-lactam antibiotics in milk and feed samples, TrAC Trends in Analytical Chemistry 28 (6) (2009) 729–744, https://doi.org/10.1016/j.trac.2009.04.005.
[39] J.H. Kang, J.H. Jin, F. Kondo, False-positive outcome and drug residue in milk samples over withdrawal times, J. Dairy Sci. 88 (2005) 908–913, https://doi.org/10.3168/JDS.S0022-0302(05)72757-0.
[40] C. Bion, A. Beck Henzelin, Y. Qu, G. Pizzocri, G. Bolzoni, E. Buffoli, Analysis of 27 antibiotic residues in raw cow's milk and milk-based products – validation of Delvotest® T AU, Food Addit. Contam. Part A 33 (2016) 54–59, https://doi.org/10.1080/19440049.2015.1104731.
[41] M.G. Papich, Cefquinome sulfate, Saunders Handb. Vet. Drugs. (2016) 133–135, https://doi.org/10.1016/B978-0-323-24485-5.00144-3.
[42] V. Pifferi, G. Cappelletti, C. Di Bari, D. Meroni, F. Spadavecchia, L. Falciola, Multi-walled carbon nanotubes (MWCNTs) modified electrodes: effect of purification and functionalization on the electroanalytical performances, Electrochim. Acta 146 (2014) 403–410, https://doi.org/10.1016/j.electacta.2014.09.099.
[43] N. Karimian, M.B. Gholivand, G. Malekzadeh, Cefixime detection by a novel electrochemical sensor based on glassy carbon electrode modified with surface imprinted polymer/multiwall carbon nanotubes, J. Electroanal. Chem. 771 (2016) 64–72, https://doi.org/10.1016/j.jelechem.2016.03.042.
[44] R. Jain, Vikas, Voltammetric determination of cefpirome at multiwalled carbon nanotube modified glassy carbon sensor based electrode in bulk form and pharmaceutical formulation, Colloids Surf. B Biointerfaces 87 (2011) 423–426, https://doi.org/10.1016/j.colsurfb.2011.06.001.
[45] F. Yañez, I. Chianella, S.A. Piletsky, A. Concheiro, C. Alvarez-Lorenzo, Computational modeling and molecular imprinting for the development of acrylic polymers with high affinity for bile salts, Anal. Chim. Acta 659 (2010) 178–185, https://doi.org/10.1016/j.aca.2009.11.054.
[46] N. Sleegers, A.L.N. van Nuijs, M. van den Berg, K. De Wael, Cephalosporin antibiotics: electrochemical fingerprints and core structure reactions investigated by LC-MSMS, Anal. Chem. 91 (3) (2019) 2035–2041, https://doi.org/10.1021/acs.analchem.8b04487 acs.analchem.8b04487.
[47] G. Camurri, P. Ferrarini, R. Giovanardi, R. Benassi, C. Fontanesi, Modelling of the initial stages of the electropolymerization mechanism of o-phenylenediamine, J. Electroanal. Chem. 585 (2005) 181–190, https://doi.org/10.1016/j.jelechem.2005.08.016.
[48] G. Kortum, Dissociation Constants of Organic Acids in Aqueous Solution, International Union of Pure and Applied Chemistry, 1961.
[49] E.P. Serjeant, B. Dempsey, Ionization Constants of Organic Acids in Aqueous Solution, (1979) 321.
[50] D. Vanossi, L. Pigani, R. Seeber, P. Ferrarini, P. Baraldi, C. Fontanesi, Electropolymerization of ortho-phenylenediamine. Structural characterisation of the resulting polymer film and its interfacial capacitive behaviour, J. Electroanal. Chem. 710 (2013) 22–28, https://doi.org/10.1016/j.jelechem.2013.04.028.
[51] H. Dai, Q. Wu, S. Sun, K. Shiu, Electrochemical quartz crystal microbalance studies on the electropolymerization processes of ortho -phenylenediamine in sulfuric acid solutions, J. Electroanal. Chem. 456 (1998) 47–59.
[52] M. Zhou, J. Heinze, Electropolymerization of pyrrole and electrochemical study of polypyrrole. Influence of acidity on the formation of polypyrrole and the multipathway mechanism, J. Phys. Chem. B 103 (1999) 8443–8450, https://doi.org/10.1021/jp990161t.
[53] M. Babaiee, M. Pakshir, B. Hashemi, Effects of potentiodynamic electropolymerization parameters on electrochemical properties and morphology of fabricated PANI nanofiber/graphite electrode, Synth. Met. 199 (2015) 110–120, https://doi.org/10.1016/j.synthmet.2014.11.012.